Lab5: Acquisition

Satellite Navigation Laboratory, Summer Semester 2022

Institute for Communications and Navigation, Technical University of Munich

Contents

1 Introduction

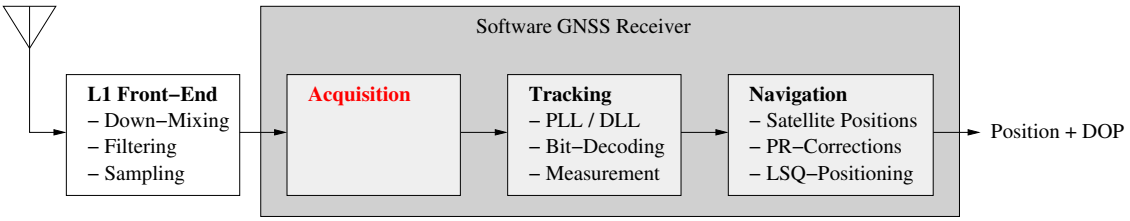

GPS satellites transmit information via analog signals with low power whose instantaneous level is lower than noise floor. Hence, proper conditioning is required for the broadcast signals at the front-end (e.g. amplification, filtering, down-converting, ADC). The processed signals are first correlated with the known chip sequences to roughly estimate signal's arrival time and the Doppler shift (not carrier phase offsets, non-coherent). This process

is called "acquisition", which we will discuss in this lab session. Using the obtained signal arrival time, we can compute pseudoranges, which are used to ultimately estimate user positions and user clock offset. In addition, user velocity and clock frequency can be estimated pseudorange rates computed with the estimated Doppler shift. Since acquisition is a global search process, big computational loads are required. Hence, once acquisition is successfully conducted, arrival time and Doppler shift (and additionally, carrier phase offset for precise positioning) are estimated by local search using the values estimated with acquisition. This process is called "tracking", and we will discuss it in the next lab session.

2 Modeling of GPS Signals

Navigation signals transmitted from GPS satellites, $s(t)$, and received signals, $r(t)$, can be modeled as

$$s(t) = \sqrt{2P_{tmt}}D(t)x(t)\cos(2\pi f_L t + \Theta_{tmt})$$
$$r(t) = \sqrt{2P_{rcv}}D(t-\tau)x(t-\tau)\cos(2\pi(f_L + f_D)t + \Theta_{rcv}) + n(t)$$

P_{tmt}, P_{rcv}	Transmitted and received power, $P_{tmt} \gg P_{rcv}$
$\Theta_{tmt}, \Theta_{rcv}$	Carrier phase of the transmitted and received signals
$D(t)$	Navigation bit sequence, $D(t) \in (-1, +1)$
$x(t)$	pseudo-random codes, chip sequence, $x(t) \in (-1, +1)$
τ	Code-phase delay (signal arrival time) [s]
f_L	RF carrier frequency [rad/s]
f_D	Doppler shift [rad/s]
$n(t)$	Additive white Gaussian noise (AWGN).

After processing the received signals at the front end, they can be modeled:

$$s(t) = \sqrt{2P_{rcv}}D(t-\tau)x(t-\tau)\cos(2\pi(f_{IF} + f_D)t + \delta\Theta) + n(t)$$

f_{IF}	Intermediate frequency [rad/s]
$\delta\Theta$	Carrier phase offset.

Note that this model is described as a continuous function of time for the sake of convenient analysis, even though signals are actually discretized after the signal processing at the front end.

For signal modulations, pseudo-random noise sequence (PRN), $x(t)$, are used with chip duration $T_c = 1/1.023\mu$s (1.023×10^6chips/s). 1023 chips build one C/A code (code duration =1ms). If there is no bit flip, 20 C/A codes can be transmitted in one Navigation bit $D(t)$ (20×1023 chips/bit, bit duration $T_b = 20$ms(50bps)). Fig. 1 roughly shows an overview of data modulation.

Using PRN, the signals from different GPS satellites can be differentiated (code division multiple access (CDMA)), which enables channel sharing and simultaneous signal transmissions from multiple satellites.

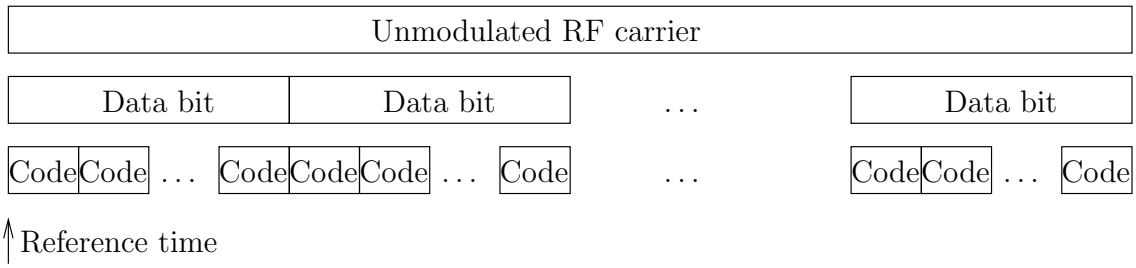

Figure 1: Modulation of GPS satellite signals with the navigation data bit and C/A codes

3 Inphase and Quadrature (IQ) Sampling and Correlation

3.1 Carrier Wipe-Off

Since we do not have a priori knowledge of carrier phase, incoming signals are modulated with both inphase and quadrature reference signals:

$$I : \sqrt{2}\cos(2\pi(f_{IF} + \hat{f}_D)t + \hat{\theta})$$
$$Q : \sqrt{2}\sin(2\pi(f_{IF} + \hat{f}_D)t + \hat{\theta}),$$

f_{IF}	Intermediate frequency [Hz]
$\hat{f}_D$	Doppler shift estimate [rad/s]
$\hat{\theta}$	Carrier phase estimate

After the modulation, the signals low-pass filtered. Then, we have inphase and quadrature signal samples:

$$I : \sqrt{P_{rcv}}D(t-\tau)x(t-\tau)\cos(2\pi\Delta f_D t + \Delta\theta)$$
$$Q : \sqrt{P_{rcv}}D(t-\tau)x(t-\tau)\sin(2\pi\Delta f_D t + \Delta\theta), \quad (1)$$

where $\Delta f_D = f_D - \hat{f}_D$ is the difference between the real Doppler shift and the estimated one, and $\Delta\theta = \delta\theta - \hat{\theta}$ is the difference between the actual carrier phase offset and the estimated input phase. After the carrier wipe-off process, the carrier frequency and intermediate frequency do not need to be considered.

3.2 Code Wipe-Off

After the carrier wipe-off process, inphase and quadrature signal samples are correlated with the known chip sequences $x(t-\hat{\tau})$, where $\hat{\tau}$ is the code-phase offset estimate. Inphase and quadrature components of the correlated signals are

$$S_I(\Delta\tau, \Delta f_D, \Delta\theta) = \frac{\sqrt{P_{rcv}}D}{T_{CO}}\int_0^{T_{CO}} x(t-\tau)x(t-\hat{\tau})\cos(2\pi\Delta f_D t + \Delta\theta)dt$$
$$S_Q(\Delta\tau, \Delta f_D, \Delta\theta) = \frac{\sqrt{P_{rcv}}D}{T_{CO}}\int_0^{T_{CO}} x(t-\tau)x(t-\hat{\tau})\sin(2\pi\Delta f_D t + \Delta\theta)dt, \quad (2)$$

where $\Delta\tau = \tau - \hat{\tau}$ is the difference between the real code-phase offset and the estimated one.

In practice, we divide the integral interval T_{CO} into several sets of interval T_i to ensure no bit boundary, i.e. navigation bit D does not change the value within at least one of the divided intervals. The first integration from 0 to T_i is called "pre-detection", which is set as $10ms$ for GPS. When the level of signals is weak (e.g. indoor navigation), the integration interval is increased as 100ms.

3.3 Ambiguity Function

The ambiguity function is the auto-correlation of the input code and generated code:

$$\tilde{R}(\Delta\tau, \Delta f_D) = \int_0^{T_{CO}} \frac{1}{T_{CO}} x(t-\tau)x(t-\hat{\tau}) \exp(j2\pi\Delta f_D t)dt. \tag{3}$$

The ambiguity function shows a clear peak with small sidelobes when the input is similar to the kernel function.

Using this ambiguity function, the correlated signals can be expressed as

$$\tilde{S} = S_I + jS_Q = \sqrt{P_{rcv}} D \exp(j\Delta\theta)\tilde{R}(\Delta\tau, \Delta f_D), \tag{4}$$

where S_I and S_Q are inphase and quadrature components described in (2), respectively.

For random codes as the GPS codes, the expectation of the ambiguity function can be derived as

$$\begin{aligned} E(\tilde{R}) &= \bar{R}(\Delta\tau)\exp(j\pi\Delta f_D T_{CO})\text{sinc}(\pi\Delta f_D T_{CO}) \\ &= \left(1 - \frac{|\Delta\tau|}{T_c}\right) \text{rect}\left(\frac{\Delta\tau}{2T_c}\right) \exp(j\pi\Delta f_D T_{CO})\text{sinc}(\pi\Delta f_D T_{CO}), \end{aligned} \tag{5}$$

where $\text{rect}\left(\frac{\Delta\tau}{2T_c}\right)$ denotes the rectangular function

$$\text{rect}\left(\frac{\Delta\tau}{2T_c}\right) = \begin{cases} 1, & \text{if } |\Delta\tau| < T_c \\ 0, & \text{otherwise} \end{cases}. \tag{6}$$

In addition, the variation of the ambiguity function for random codes is

$$\text{var}(\tilde{R}) = \begin{cases} \left(\frac{\tau}{T_c}\right)^2 \frac{1}{N}, & \text{if } -T_c < \tau < T_c \\ \left(\frac{\tau - iT_c}{T_c}\right)^2 \frac{1}{N} + \left(\frac{(i+1)T_c - \tau}{T_c}\right)^2 \frac{1}{N}, & \text{if } iT_c < \tau < (i+1)T_c; i \neq (-1, 0) \end{cases}, \tag{7}$$

which shows that the peak of the ambiguity function is sharper when the number of the chip sequences in one C/A code N is larger.

4 Non-Coherent Acquisition Methods

In practice, the squared magnitude of the ambiguity function $|\tilde{R}|^2$ is examined to ignore the influence of navigation bit D and carrier phase offset $\Delta\theta$. Additionally, the exponential kernel $\exp(j\Delta\theta)$ in (4) can be ignored, assuming non-coherent acquisition. Hence, we only need to estimate code-phase delay ($\hat{\tau}$) and Doppler shift ($\hat{f_D}$) that maximize $|\tilde{R}|^2$. In this section, three representative non-coherent acquisition approaches are explained.

4.1 Serial Search

As depicted in Fig. 2, serial search is a brute-force algorithm that examines $|\tilde{R}|^2$ with all possible combinations of code-phase delay and Doppler shift for each known C/A code. Fig. 3 shows a block diagram of search search.

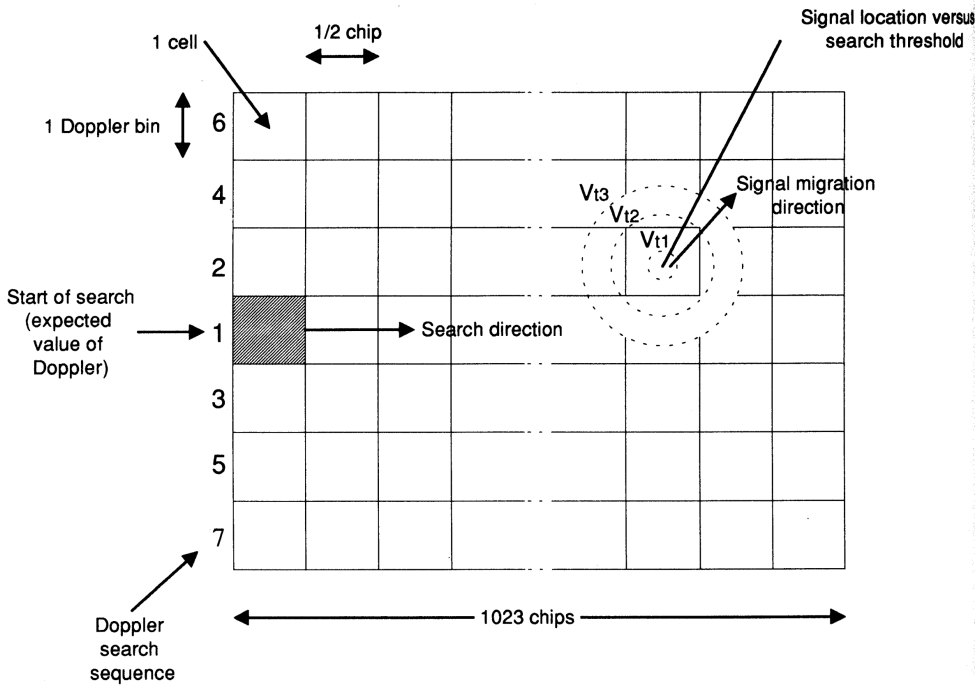

Figure 2: Two dimensional search grids for a non-coherent serial search for one C/A code. The search process needs to be repeated for all possible C/A codes (PRN sequences) [1].

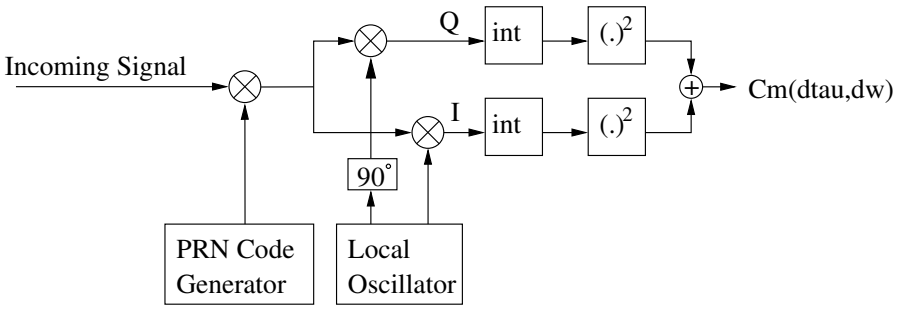

Figure 3: A block diagram of non-coherent serial search

4.2 Parallel Frequency Space Search

For a faster search, parallel frequency space search examines Doppler shifts in parallel for each code-phase offset candidate, by using the discrete Fourier transform (DFT) for each code delay. Fig.4 shows a flowchart of non-coherent parallel frequency space search. To reduce computational loads, the fast Fourier transform (FFT) can be applied to conduct the DFT.

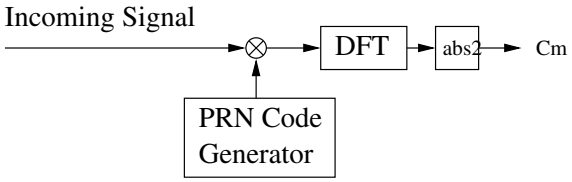

Figure 4: A block diagram of non-coherent parallel frequency space search

4.3 Parallel Code Space Search

In parallel code space search, we examines code-phase offsets in parallel for each Doppler shift candidate to make the algorithm faster. As depicted in Fig.5, first, the IQ components of incoming signals are converted to the frequency domain with FFT:

$$I(t) + jQ(t) = x(t)\cos(\omega_c t) + jx(t)\sin(\omega_c t) = x(t)\left(\cos(\omega_c t) + j\sin(\omega_c t)\right) = x(t)e^{j\omega_c t}$$

PRN codes are also converted to the frequency domain using a FFT. After converting them to the frequency domain, the signals and PRN codes are correlated, then they are converted back to the time domain with the inverse FFT (IFFT).

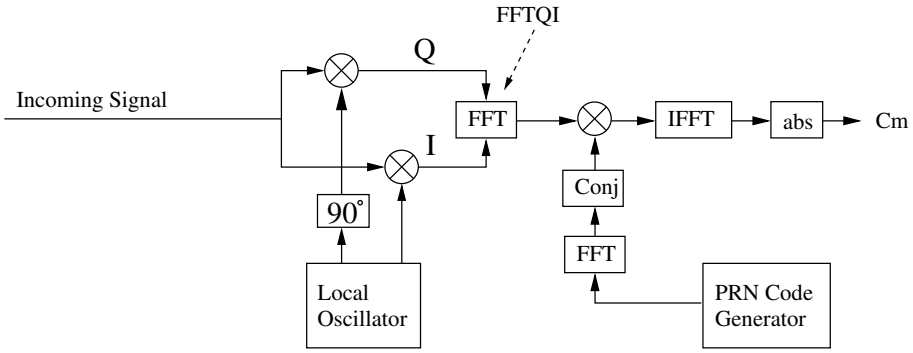

Figure 5: A block diagram of non-coherent parallel code phase search

References

[1] E. Kaplan and C. J. Hegarty, *Understanding GPS: Principles and Applications, Second Edition.* Artech House, 2006.

[2] P. Misra and P. Enge, "Global positioning system: signals, measurements and performance second edition," *Massachusetts: Ganga-Jamuna Press*, 2006.

[3] C. Günther, *Satellite Navigation.* Insitute for Communications and Navigation, Technical University of Munich, 2017.

[4] F. Johansson, R. Mollaei, J. Thor, and J. Uusitalo, "GPS satellite signal acquisition and tracking," tech. rep., LuleåUniversity of Technology, 1998.

[5] GPS Navstar JPO, *ICD-GPS-200C, Navstar GPS Space Segment/Navigation User Interfaces.*

5 Homework

1. Determine a proper search grid size of code-phase delay and Doppler shift to find the maximum expectation of the ambiguity function (5) for the following two cases:
   a) Perfect spreading-code synchronization ($\Delta\tau = 0$)
   b) Perfect carrier-frequency synchronization ($\Delta\omega = 0$)

   Assume that an integration period is 1ms, and at least 1/2 of the maximum expectation (5) should be visible in the search grids.

2. First, define the following parameters
   - The number of samples per integration interval N
   - The number of bins for the code-phase offset search m
   - The number of bins for the Doppler shift search n

   with the integration interval T_i, sampling frequency f_s, the maximum Doppler shift $f_{D,max}$, Doppler spacing Δf_D, and the code-phase spacing $\Delta\tau$. Then, compare complexity of the three search methods discussed in Section 4, using *Big-O Notation* and N, m, n.

3. Express the resolutions of the frequency and code phase grids (Δf_D and $\Delta\tau$) of the two parallel search methods introduced in Section 4, using the sampling frequency f_s and the number of samples per integration interval N.

4. What is needed to use the GPS signal for navigation with meter-level accuracy? What would be the main difference between the GPS L1 band raw spectrum (center frequency 1.57542GHz, bandwidth 1MHz) and the GSM service downlink signal (frequency band from 1.805 to 1.880GHz)?

6 Lab Tasks*

*You can find the sampling and intermediate frequency in `testIFdata.txt`, as well the expected results.

1. **Serial search:** First, adjust the Doppler and code-phase spacing in `initSettings.m`.

   Then, implement the serial search algorithm in `serialsearch.m`.
   Check the computed correlation values with figures. When the tested PRN is same as the one of the received signal, the graph will be similar as Fig. 6a, where a clear peak exists. Otherwise, no peak will be detected as Fig. 6b.
   In addition, examine the ratio of the first and second maximum of the correlation values. If this ratio is higher enough with the PRN k, set the `channels` struct as

   - `channels.PRN(`k`)=1`
   - `channels.carrFreq(`k`)=` $f_{IF} + f_D$
   - `channels.codePhase(`k`)=` τ

   The implemented code can be executed with `channels = gpsAcquisition(IF_recordings_file, sampling_frequency, intermediate_frequency)`.

2. **Serial search with two integral intervals:** To guarantee no bit boundary in an integration interval, we need to divide the total integral interval into two in practice. Extend `serialsearch.m` by dividing the total interval into two, and compute the correlation for each interval.

3. **Parallel frequency space search:** Implement parallel frequency space search in `pfssearch.m`,

   The function can be run with `channels = gpsAcquisition(IF_recordings_file, sampling_frequency, intermediate_frequency)`. Before executing this function, modify the line 45 in `gpsAcquisition.m`.

4. **Parallel code space search:** Implement parallel code space search in `pcssearch.m`.

   The implemented code can be executed with `channels = gpsAcquisition(IF_recordings_file, sampling_frequency, intermediate_frequency)`. Modify line 45 in the function before the execution.

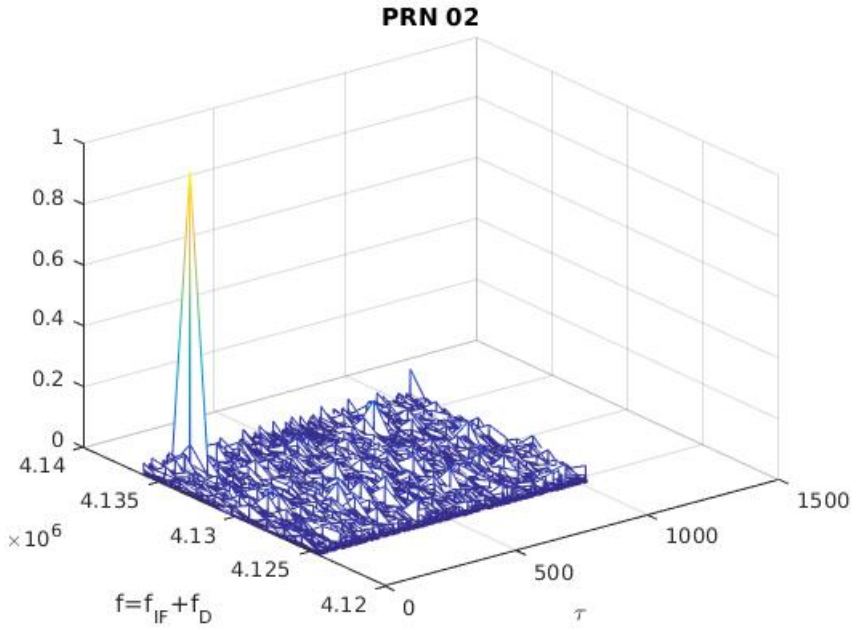

(a) A clear peak exists with sidelobes since the current PRN sequence is found in the received signals.

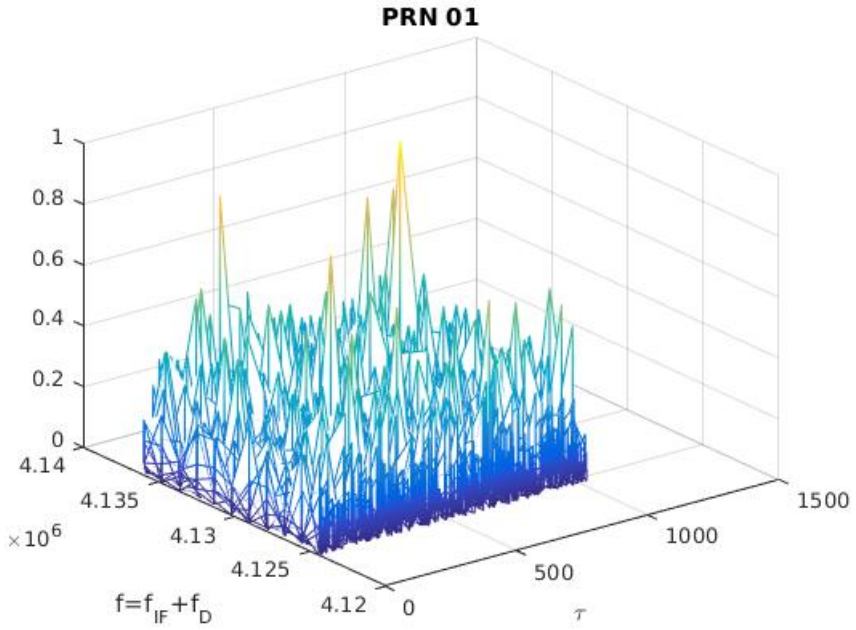

(b) A clear peak does not exist since the current PRN is not found in the received signals.

Figure 6: C_m of observable and non-observable PRNs